



Chemical composition and mixing state of BC-containing particles and the implications on light absorption enhancement

Jiaying Sun^{1,2}, Yele Sun^{1,2,3}, Conghui Xie^{1,2, a}, Weiqi Xu¹, Chun Chen^{1,2}, Zhe Wang¹, Lei Li⁴, Xubing
5 Du^{4,5}, Fugui Huang⁶, Yan Li^{1,2}, Zhijie Li^{1,2}, Xiaole Pan¹, Nan Ma⁷, Wanyun Xu⁸, Pingqing Fu⁹, and Zifa
Wang^{1,2,3}

¹State Key Laboratory of Atmospheric Boundary Layer Physics and Atmospheric Chemistry, Institute of Atmospheric Physics,
Chinese Academy of Sciences, Beijing 100029, China

10 ²College of Earth and Planetary Sciences, University of Chinese Academy of Sciences, Beijing 100049, China

³Center for Excellence in Regional Atmospheric Environment, Institute of Urban Environment, Chinese Academy of Sciences,
Xiamen 361021, China

⁴Institute of Mass Spectrometer and Atmospheric Environment, Jinan University, Guangzhou, 510632, China

15 ⁵Guangdong Provincial Engineering Research Center for On-Line Source Apportionment System of Air Pollution, Guangzhou,
510632, China

⁶Guangzhou Hexin Analytical Instrument Company Limited, Guangzhou, 510530, China

⁷Institute for Environmental and Climate Research, Jinan University, Guangzhou 511443, China

⁸State Key Laboratory of Severe Weather & Key Laboratory for Atmospheric Chemistry, Institute of Atmospheric
Composition, Chinese Academy of Meteorological Sciences, Beijing, 100081, China

20 ⁹Institute of Surface-Earth System Science, Tianjin University, Tianjin 300072, China

^anow at: State Key Joint Laboratory of Environmental Simulation and Pollution Control, College of Environmental Sciences
and Engineering, Peking University, Beijing, 100871, China

Correspondence: Yele Sun (sunyele@mail.iap.ac.cn)



Abstract. The radiative forcing of black carbon (BC) depends strongly on its mixing state in different chemical environments. Here, we analyzed the chemical composition and mixing state of BC-containing particles by using a single particle aerosol mass spectrometer and investigated their impacts on light absorption enhancement (E_{abs}) at an urban (Beijing) and a rural site (Gucheng) in North China Plain. While the BC was dominantly mixed with organic carbon (OC), nitrate and sulfate at both urban and rural sites, the rural site showed much higher fraction of BC coated with OC and nitrate (36% vs. 15 – 20%). Moreover, the BC mixing state evolved significantly as a function of relative humidity with largely increased coatings of OC-nitrate and nitrate at high RH levels. By linking with the bulk composition of organic aerosol (OA), we found that the OC coated on BC comprised dominantly secondary OA in Beijing, while primary and secondary OA were similarly important in Gucheng. Furthermore, E_{abs} was highly dependent on the secondary inorganic aerosol coated on BC at both sites, while the coated primary OC also resulted in an E_{abs} of ~ 1.2 for relatively fresh BC particles at the rural site. Positive matrix factorization analysis was performed to quantify the impact of different mixing state on E_{abs} . Our results showed the small E_{abs} (1.06 \sim 1.11) for BC particles from fresh primary emissions, while the E_{abs} increased significantly above 1.3 when BC was aged rapidly with increased coatings of OC-nitrate or nitrate, and it can reach above 1.4 as sulfate was involved in BC aging.

1 Introduction

Black carbon (BC), also referred to soot and element carbon, contributes a substantial and positive impact on climate radiative forcing (Bond et al., 2013; IPCC, 2013). High loading of atmospheric BC could depress the development of planetary boundary layer and aggravate the haze pollution episodes (Ding et al., 2016). However, accurate estimation of light absorption and radiative forcing of BC is still challenging due to its complex emission sources (e.g., fossil fuel and biomass burning) and microphysical properties (e.g., mixing state and coating composition) (Kahnert, 2010; Vignati et al., 2010; Liu et al., 2017; Cappa et al., 2019). Light absorption of BC is composed of pure BC absorption and the enhanced light absorption (E_{abs}) induced by "lensing effect", which is due to the chemical materials coated on BC (Fuller et al., 1999; Bond and Bergstrom, 2006; Lack and Cappa, 2010). In order to determine the E_{abs} , the thermodenuder (TD)-method (Liu et al., 2015; Zhang et al., 2016), mass absorption efficiency (MAE)-method (Wang et al., 2014; Zhang et al., 2018) and Mie theoretical calculations (Liu et al., 2017)



are widely used in previous studies. However, the E_{abs} in different chemical environments is considerably different, such as the negligible E_{abs} (1.06) in California while a significant light absorption enhancement (~ 1.8) in Kanpur (Cappa et al., 2012; Thamban et al., 2017). One explanation is due to the variety of mixing state of BC from different sources, urban and rural
50 background sites, and aging processes (Liu et al., 2015; Liu et al., 2017).

Extensive studies have been conducted to characterize the mixing state of BC (Li et al., 2016b). Buseck et al. (2014) used the transmission electron microscopy (TEM) to determine the size, morphology, mixing state and chemical compositions of soot particles, and Li et al. (2016a) used the same technique for characterization of size and aging dependent mixing state of individual particles in both clean and polluted environment in China. More recently, the development of soot particle aerosol
55 mass spectrometer (SP-AMS) is able to measure refractory BC (rBC) and coated aerosol species in real-time (Lee et al., 2015). For example, Xie et al. (2019a) found that secondary organic and inorganic components contributed mostly to the coating materials of rBC in summer, while Liu et al. (2019) reported that rBC was more mixed with primary organic components (e.g., coal combustion and biomass burning) than secondary species in winter. Comparatively, more comprehensive mixing state of BC particles and the chemical compositions of coatings could be acquired by aerosol time-of-flight mass spectrometry
60 (ATOFMS) or single particle aerosol mass spectrometer (SPA-MS) (Pratt and Prather, 2012). A recent study in winter in North China Plain (NCP) showed that most of BC particles were mixed with sulfate and organic carbon (OC) due to the intensive coal combustion and biomass burning emissions in heating period (Chen et al., 2020b; Wang et al., 2020), while BC particles were more mixed with nitrate in summer in Beijing (Xie et al., 2020). Although the mixing state, coating compositions and E_{abs} of BC have been widely discussed in previous studies, our understanding of BC properties in winter particularly the
65 differences between urban and rural areas in NCP are limited.

In this study, we deployed a newly developed high resolution single particle aerosol mass spectrometer (Zhu et al., 2020), and a photoacoustic extinctions (PAX) coupled with a thermodenuder at an urban and a rural site in NCP to investigate the mixing state of BC-containing particles and its relationship with light absorption enhancement. Meanwhile, the aerosol bulk composition was measured simultaneously by a high-resolution aerosol mass spectrometer (HR-AMS). The chemical
70 composition and mixing state of BC-containing particles are characterized, and the evolution of BC mixing state and the



driving factors are investigated. Finally, the impacts of the changes in mixing state of BC on light absorption enhancement and radiative forcing are elucidated.

2 Methods

2.1 Sampling sites and measurements

75 The measurements were conducted at an urban site from 18 October to 1 December, 2019 and a rural site from 9 December 2019 to 13 January 2020. The urban site is located at the Institute of Atmospheric Physics (IAP), Chinese Academy of Sciences (39°58'28"N, 116°22'16"E) in Beijing (BJ). The rural site of Gucheng (GC) in Hebei province is located ~120 km to the southwest of Beijing. Ambient aerosols with a flow rate of 3 L min⁻¹ were drawn into a PM_{2.5} cyclone (Model: URG-2000-30ED) and a nafion dryer, then aerosol particles (~2 L min⁻¹) were sampled by switching between the thermodenuder (TD) and bypass line (BP) every 15 min into a HR-AMS to measure non-refractory submicron aerosol (NR-PM₁) species and a PAX (Droplet Measurement Technologies) for absorption [$b_{\text{abs}}(\lambda)$] and scattering [$b_{\text{sca}}(\lambda)$] coefficients at 870 nm. Note that equivalent BC (eBC) is converted from $b_{\text{abs}}(\lambda)$ into mass concentration with a reference mass absorption efficient (MAE_{ref}, 4.44 m² g⁻¹ in this study (Bond and Bergstrom, 2006)). A complete TD cycle took 150 minutes, during which the temperature increased gradually from 25°C to 250 °C followed by a 15 min cooling down to 25°C. E_{abs} was then calculated as the ratio of ambient BC particle absorption ($b_{\text{abs, total}}$) to that thermodenuded (considered as pure BC absorption) when temperature was higher than 200°C ($b_{\text{abs, BCpure}}$). More detailed description of the measurements and methods could be found in a previous study (Sun et al., 2021).

The mixing state and chemical composition of single particles are detected by a high-resolution single particle aerosol mass spectrometer (HR-SPAMS, Hexin Analytical Instrument Co., Ltd.). The aerodynamic diameters of single particles are determined from the velocity detected by two continuous laser beams (diode Nd: YAG, 532 nm). After passing through the sizing region, particles are desorbed and ionized by a pulsed Nd: YAG laser (266 nm), and the positive and negative fragments are detected by a Z-shaped bipolar time-of-flight mass spectrometer to inform the chemical compositions. A more detailed description of the SPA-MS can be found elsewhere (Li et al., 2011). Compared with the traditional SPA-MS, the new HR-



SPAMS uses a new aerosol concentration sampling device and improves the transmission efficiency of coarse particles. Meanwhile, a delayed extraction technology is introduced to improve the mass resolution and increase the hit rate by a factor of 2 ~ 4 for ambient particles (Chen et al., 2020c). Also, the ion signals with high and low intensity are separated by multichannel acquisition technology and detected simultaneously, which makes the system dynamic range more than 40 times of the traditional data acquisition system and improves the detection of ions with low signals greatly (Shen et al., 2018; Zhong et al., 2021).

100 2.2 Data analysis

In total, 3 619 038 and 4 655 426 particles were analyzed in Beijing and Gucheng, respectively. The size and chemical composition of each single particle is informed by Computational Continuation Core (COCO) toolkit in MATLAB software. Based on the marker of C_n^\pm ($n = 1, 2, 3, \dots$) clusters, 2 269 659 and 3 399 565 BC-containing particles are identified in Beijing and Gucheng, respectively. Four typical sources of BC-containing particles are further identified according to the characteristic ion markers: (1) particles containing abundant signals of $39[K]^+$, $45[CHO_2]^-$ and $59[C_2H_3O_2]^-$ or $73[C_3H_5O_2]^-$ with the peak areas more than 0.5% are classified as BB_{pure} type from biomass burning (Silva et al., 1999; Healy et al., 2010); (2) particles containing abundant signals of $7[Li]^+$, $23[Na]^+$, $27[Al]^+$, $43[AlO]^-$, $80[SO_3]^-$, $97[H_2SO_4]^-$ and polycyclic aromatic hydrocarbons are classified as CC_{pure} type from coal combustion (Zhang et al., 2009; Healy et al., 2010); (3) particles containing abundant signals of $40[Ca]^+$, $51[V]^+$, $55[Mn]^+$, $67[VO]^+$, $46[NO_2]^-$, $62[NO_3]^-$ and $79[PO_3]^-$ are classified as TR_{pure} type from traffic emissions (Yang et al., 2017); (4) particles internally mixed with more than one source (three sources above) are unified together and named as Mix_{Source} type. The BC-containing particles above are collectively referred to BC_{fresh} . The remain BC-containing particles are named BC_{aged} and classified by using the ART-2a algorithm with a vigilance factor of 0.75, a learning rate of 0.05 and 20 iterations (Song et al., 1999). Seven particle types are grouped and named based on two principles: (1) the particles are named BCOC when the signals of $37[C_3H]^+$, $43[C_2H_3O]^+$, $51[C_4H_3]^+$ and $63[C_5H_3]^+$ are comparable with C_n^+ in positive ion area (Healy et al., 2012; Xie et al., 2020), otherwise they are named BC; (2) On the basis of (1), the particles are named $BCOC_N$ or $BCOC_S$ when they are only mixed significantly with nitrate ($46[NO_2]^-$ and $62[NO_3]^-$) or sulfate ($97[H_2SO_4]^-$)



). Otherwise, they are named BCOC_{NS} when they present comparable peak areas of nitrate and sulfate. The more detailed names of BC-containing particle types are shown in Table S1.

The sources of bulk OA were analyzed by positive matrix factorization (PMF) and five OA factors were identified at both
120 urban and rural sites, including biomass burning OA (BBOA), fossil fuel-related OA (FFOA), cooking OA (COA), less
oxidized oxygenated OA (LO-OOA) and more oxidized OOA (MO-OOA) in Beijing and BBOA, coal combustion OA
(CCOA), hydrocarbon-like OA (HOA), OOA and aqueous-related OOA (aq-OOA) in GC (Table S1). The detailed PMF
analysis of OA in Beijing and Gucheng are presented Xu et al. (2021) and Chen et al. (2021). The PMF analysis was also
performed to identify the effect of different mixing state on E_{abs} , by inputting $b_{\text{abs, total}}$, $b_{\text{abs, BCpure}}$ and 11 major types of BC-
125 containing particles derived from HR-SPAMS. The detailed pre-treatment of error matrix, and the selection of factor solutions
could be found in previous studies (Petit et al., 2014; Xie et al., 2019b). Then, the E_{abs} of each factor can be calculated as the
ratio of $b_{\text{abs, total } f_i}$ and $b_{\text{abs, BCpure } f_i}$ in factor i .

3 Results and discussion

3.1 BC-containing particles at urban and rural sites

130 BC-containing particles on average accounted for 62% of the total particles in Beijing, lower than that in Gucheng (73%) and
higher than that in winter 2018 in Beijing (55%) (Xie et al., 2020). Similarly, a previous winter study in Beijing also found
that 60 – 78% of aerosol particles contained BC (Chen et al., 2020a). According to Figs. 1 and S1, we found that the mass
spectra of BC-containing particles at the two sites are somewhat similar which are both characterized by C_n^\pm ($n = 1-7$),
27[C₂H₃]⁺, 37[C₃H]⁺, 43[C₂H₃O]⁺, 51[C₄H₃]⁺ 63[C₅H₃]⁺, 46[NO₂]⁻, 62[NO₃]⁻ and 97[HSO₄]⁻ peaks, indicating that BC-
135 containing particles are consistently mixed with OC, nitrate (NO₃) and sulfate (SO₄) at the rural and urban sites. Comparatively,
more than 80% of BC-containing particles are internally mixed with SO₄ in Beijing while those in Gucheng accounted for less
than 60%, suggesting that BC particles were more aged at the urban site. In addition, approximately 40% of BC-containing
particles was mixed with amines (e.g., 59[(CH₃)₃N]⁺ and 74[(C₂H₅)₂NH₂]⁺) in GC, which is twice than that in BJ. One



140 explanation is the more nitrogen-containing compounds formed from either aqueous-phase processing due to higher RH (69% vs. 45%) or biomass burning emissions at the rural site (Zhang et al., 2012; Chen et al., 2019).

The study in Beijing was divided into two periods, i.e., non-heating period (BJ-NHP) from 28 October to 10 November and heating period (BJ-HP) from 10 November to 1 December, while the observation in Gucheng was performed during heating period. As illustrated in Fig. 2a, the BC-containing particles are dominantly contributed by BC_N and $BCOC_N$ (~20%) during BJ-NHP, indicating that BC was mainly internally mixed with nitrate at the urban site. Compared with BJ-NHP, the fractions
145 of $BCOC_S$ and Mix_{Source} increased significantly during BJ-HP, especially during relatively clean periods, suggesting a considerable change in BC mixing state from non-heating to heating period due to the enhanced primary emissions, e.g., coal combustion. Previous studies showed that BC was mainly mixed with sulfate in winter in Beijing (Chen et al., 2020b; Xie et al., 2020), while this study showed a dominant mixing of BC with nitrate. This was likely due to the fact that coal fuels in Beijing were replaced by clean energies, e.g., natural gas and electricity after 2017 (Zhang et al., 2019). Indeed, the changes
150 in nitrate concentrations were relatively small in winter in Beijing since clean air action although the sulfate concentrations showed large decreases (Zhou et al., 2019; Lei et al., 2020). Comparatively, $BCOC_N$ was the major BC-containing particle type accounting for 36% in GC, which was twice than that in BJ-HP indicating that BC particles were dominantly mixed with OC and nitrate in an environment with high RH and intensive primary emissions, e.g., coal combustion emissions. In addition, BB_{pure} and TR_{pure} showed pronounced diurnal cycles in GC (Fig. S2) compared with the relatively flat diurnal variations of
155 BB_{pure} in BJ, suggesting intensive biomass burning and diesel vehicle emissions at the rural site especially nighttime.

3.2 Chemical composition and mixing state in different environment

Figure 3 shows the variations of number fractions of different BC-containing types under different RH levels in BJ and GC. Almost all BC_{aged} types showed strong dependence on RH while the number fractions of BC_{fresh} types decreased with increasing RH at both sites indicating that high RH environment was more favorable for BC aging (Zhang et al., 2021). Similar to BC_{fresh} ,
160 $BCOC_S$ was the only type of aged BC showing decreased fraction as a function of RH in BJ and GC. In fact, the high correlations between $BCOC_S$ and CC_{pure} ($R^2 = 0.89$ and 0.98 , in BJ and GC, respectively) highlight that BC emitted from coal combustion could be directly mixed with OC and SO_4 at low RH level, and evolve towards the mixing with OC and NO_3 under



high RH conditions. Moreover, the number fraction of BC_N increased gradually as the increase of RH and dominated BC particles (~30%) at RH = 90 – 100% in BJ, suggesting that the newly formed nitrate that coated on fresh BC played an important
165 role in the formation of severe pollution in urban region. Comparatively, the number fraction of $BCOC_N$ increased the most by 43%, accounting for more than half of BC-containing particles at high RH levels in GC. This result indicates that the type of $BCOC_N$ was more important to aggravate air pollution in rural area. In addition, we found that the fraction of $BCOC_{NS}$ decreased obviously as a function of RH in GC indicating the impact of the transition from photochemical production to aqueous-phase reactions on the mixing state of BC. This result also suggests that aqueous-phase formation of sulfate at high
170 RH level appeared not to affect BC mixing state substantially, consistent with previous studies that aqueous-phase processing did not affect the total E_{abs} in GC (Sun et al., 2021; Zhang et al., 2021). However, $BCOC_{NS}$ in BJ showed relatively stable fractions across different RH levels suggesting the different sources from the rural site.

Figure 3 shows the evolution of mixing state of BC-containing particles during two different haze events in Beijing. During the initial stage of haze episode (P0), the contribution of $BCOC_S$ started to decrease while the number fraction of $BCOC_N$
175 increased significantly. As a consequence, E_{abs} increased rapidly from ~1.1 to 1.3 in half day. Then, the number fraction of BC_N increased while that of BC_{fresh} decreased during P1 period. These results indicated that fresh BC was gradually aged by mixing with nitrate during the evolution of haze episode. BC_N increased continually during P2 with high E_{abs} up to 1.4, and finally the mixing state of BC was stabilized as indicated by the relatively stable number fractions of most BC particle types and small changes in E_{abs} . Similar to haze episode 1, the freshly emitted BC was gradually mixed with nitrate and OC causing
180 high E_{abs} (up to 1.5) during P3 and P4. As shown in Fig. 3d, the sources of fine particles were dominated by fossil fuel OA and presented strong diurnal variations due to the influences of mountain valley winds. As a result, E_{abs} also presented a pronounced diurnal cycle with higher values during daytime, indicating that the different air masses brought by the mountain valley winds affected BC mixing state and light absorption enhancement. The number fraction of BC_N increased significantly during the severest polluted period (P5) associated with simultaneous increases in BBOA, indicating the mixing of BC from biomass
185 burning with nitrate under high RH and PM levels, and hence E_{abs} was comparably high (1.35). After the P5 period, the BBOA was relatively stable and FFOA increased significantly. Correspondently, the proportion of $BCOC_N$ in BC is higher, indicating that fresh BC emitted from fossil fuel emission was likely mixed with OC and nitrate at high PM level. Different from Beijing,



the evolution of BC mixing state during most haze events were similar in GC (Figs. 2c and S3), which was characterized by most significant increase in BCOC_N rather than BC_N as the PM increased. Moreover, BCOC_N particles were increased more significantly during nighttime while BCOC_{NS} was more significant during daytime. Such differences were mainly due to the enhanced coal combustion pollutants at nighttime (Fig. S2) which were mixed with photochemical products during daytime. Overall, our results suggest that the fresh BC particles from biomass burning emissions are more directly mixed with nitrate under high RH conditions, and then mixed with more sulfate during further aging. Comparatively, the fresh BC particles from coal combustion are often mixed with OC and sulfate first, and then mix further with OC and nitrate at high RH level. In addition, our results also demonstrate that the E_{abs} in GC was largely due to coal combustion emissions internally mixed with OC, consistent with our previous study showing a large impact of coal combustion emissions on E_{abs} (Sun et al., 2021).

3.3 Effects of chemical composition on E_{abs}

As shown in the average positive mass spectra of total BC-containing particles (Fig. S2), the peak areas of C_n^+ , OC and metal contributed more than 95% to the total peak area, while the peak areas of NO_3 ($46[\text{NO}_2]^-$ and $62[\text{NO}_3]^-$) and SO_4 ($97[\text{HSO}_4]^-$) accounted for more than 80% in the negative mass spectra. To better characterize the relationship between chemical species and E_{abs} , we summed C_n^\pm ($n=1\sim 5$, accounting for more than 99% in C_n) peak areas to represent BC and the total of NO_3 and SO_4 peak areas to represent secondary inorganic components coated on BC. In addition, the sum of positive peak areas except C_n^+ was defined as OC + Metal to represent the OC and metal components coated on BC. These peak areas covered almost all of the chemical components coated on BC in total BC-containing particles.

Figures 4a and 4b show the relationship between peak area ratios (measured by SPAMS) and mass concentration ratios (measured by HR-AMS) in Beijing and Gucheng, respectively. As the increase of $(\text{NO}_3 + \text{SO}_4)_{\text{AMS}}/\text{eBC}$ mass concentration ratio, the $(\text{NO}_3 + \text{SO}_4)/\text{C}_n$ peak area ratio increased first and then gradually became stable at both sites. These results indicated that BC was rapidly aged and internally mixed with secondary inorganic components during the early stage of haze episode, and appeared to be fully aged when the ratio of NO_3 and SO_4 to eBC exceeded ~ 6 . Different from secondary inorganic species, the peak area ratio of $(\text{OC} + \text{Metal})/\text{C}_n$ showed a high dependence on the mass concentration ratio of POA (e.g., the sum of BBOA and FFOA in BJ and the sum of BBOA, CCOA and HOA in GC) to eBC at both sites. Moreover, the mass concentration



ratio of SOA/eBC also presented a high correlation with $(OC + Metal)/C_n$ in BJ ($R^2 = 0.81$) and GC ($R^2 = 0.95$). We then used multiple linear regression analysis to quantify the impacts of POA and SOA on BC-coated OC. Our results showed that the average contribution of SOA to the coated OC was nearly twice that of POA (65% vs. 35%) in Beijing, while POA and SOA
215 contributed similarly in Gucheng.

$$y = 0.93 * (1 - e^{-0.62*x}) \quad (1)$$

$$y = 0.85 * (1 - e^{-0.71*x}) \quad (2)$$

$$\frac{OC+Metal}{C_n} = 0.61 * \frac{POA}{eBC} + 0.60 * \frac{SOA}{eBC} \quad (3)$$

$$\frac{OC+Metal}{C_n} = 0.78 * \frac{POA}{eBC} + 0.41 * \frac{SOA}{eBC} \quad (4)$$

220 Figures 4c and 4d show the relationship between E_{abs} and the ratio of coating materials to C_n in Beijing and Gucheng, respectively. Light absorption enhancement showed strong dependence on $(NO_3 + SO_4)/C_n$ at both sites yet the changes in E_{abs} appeared independent of $(OC + Metal)/C_n$. As shown in Fig. 4c, the ratio of $(OC + Metal)/C_n$ still presented high values at $E_{abs} = \sim 1$, while the secondary species coated on BC were negligible. These results suggested OC and metals were likely either filled internal void spaces of fresh BC or mainly externally mixed with BC which did not induce light absorption enhancement
225 at the urban site. As the progress of aging, E_{abs} increased significantly mainly due to the increased secondary coating materials. Similar to Beijing, E_{abs} also increased significantly as a function of $(NO_3 + SO_4)/C_n$ in Gucheng. The difference is the high background E_{abs} of ~ 1.20 in GC when the $(NO_3 + SO_4)/C_n$ ratio was closed to 0. Combined with the peak area ratio of $(OC + Metal)/C_n$ was about 2.5 at that time, we found that OC and metals were not only as filler materials but also coated on fresh BC and induced light absorption enhancement at the rural site. After the further aging process in atmosphere, E_{abs} was mainly
230 due to the increased secondary inorganic components coated on BC. Considering that the measurements of BC mixing state by SPAMS are often not available in field campaigns, we predicted the E_{abs} by using Eqs. 1 – 6 with aerosol species measured by AMS. The predicted E_{abs} showed overall agreements with the measured values in both BJ and GC, yet the variations at specific $NR-PM_1/eBC$ were much smaller (Fig. S4). We also estimated the E_{abs} in summer 2017 using the same method and



compared with the measurements by a TD-CAPS (Fig. S4). Our results showed that the average E_{abs} in summer was 1.24,
235 which was close to the average about 1.2 reported by Liu et al. (2019), yet higher than that in Xie et al. (2019a).

$$E_{abs} = 0.29 * \frac{NO_3+SO_4}{C_n} + 0.02 * \frac{OC+Metal}{C_n} + 1 \quad (5)$$

$$E_{abs} = 0.15 * \frac{NO_3+SO_4}{C_n} + 0.08 * \frac{OC+Metal}{C_n} + 1 \quad (6)$$

3.4 Effects of mixing state on E_{abs}

The PMF analysis is used to characterize the effects of different mixing state on E_{abs} (Fig. 5). Note that E_{abs} was not estimated
240 when the factor contributed negligibly to the total BC, such as Factor5 in BJ. As illustrated in Fig. 5, Factor2 is the major type
of aged BC in the urban region, accounting for more than 60% of the total BC. This factor was dominated by BC_N , $BCOC_N$,
 $BCOC_{NS}$ and BC_{NS} , and presented a high E_{abs} of 1.38. Comparatively, FactorB is the major type of aged BC in the rural area
which was dominated by $BCOC_N$. The E_{abs} was ~ 1.35 for this factor, which was comparable to that in BJ. As this factor evolved
towards FactorA after further aging and internally mixed with a large amount of sulfate, E_{abs} was increased up to 1.41. In
245 Beijing, the relatively fresh traffic emissions are dominant in Factor4 which showed a negligible impact on light absorption
enhancement (~ 1.06), consistent with the results in previous studies (Liu et al., 2017; Sun et al., 2021). Compared with traffic
emissions, the relatively fresh biomass burning and coal combustion emissions (Factor3) comprising mainly Mix_{Source} and
 $BCOC_S$ showed a moderate E_{abs} (~ 1.11) in BJ. Although the mixed fresh primary emissions (FactorD) in GC presented a
relatively low E_{abs} (1.06), we found that the FactorC from coal combustion emissions and mixed with much OC and nitrate
250 showed a much higher E_{abs} (~ 1.31) than that in BJ (Factor3). After more aging, more sulfate could be internally mixed with
BC and enhanced the E_{abs} , such as Factor1 with E_{abs} up to 1.42. Overall, E_{abs} shows a similar dependence on the evolution of
mixing state of BC-containing particles at urban and rural sites, i.e., fresh BC particles from primary emissions (e.g., biomass
burning, coal combustion and traffic) showed the small E_{abs} (1.06~1.11). At relatively high RH level, BC could be directly
mixed with nitrate or OC-nitrate (BC_N and $BCOC_N$), accounting for more than 60% of BC, and lead to an increase in E_{abs}



255 above 1.30; and then, the BC-containing particles were further mixed with sulfate (BC_{NS} and $BCOC_{NS}$) after continuous aging in atmosphere, and resulted in the highest E_{abs} above 1.40.

Based on E_{abs} for each factor and its contribution to $b_{abs, BC_{pure}}$, we estimated the direct radiative forcing (ΔF_R) caused by BC-containing particles with their mixing state at the top-of-atmosphere (TOA) (Chylek and Wong, 1995; Chen and Bond, 2010). The detail descriptions for the estimation are presented in supplementary. As shown in Fig. 5, the ΔF_R caused by pure BC
260 particles is about $+0.43 \text{ W m}^{-2}$ and $+0.60 \text{ W m}^{-2}$ in Beijing and Gucheng, respectively. Considering the mixing state of BC, ΔF_R could increase to 0.59 W m^{-2} and 0.82 W m^{-2} in Beijing and Gucheng, respectively. Our results demonstrated that the mixing state of BC-containing particles can have a large impact on radiative forcing estimation by up to 27%.

4 Conclusions

HR-SPAMS, TD-PAX and HR-AMS were deployed at the urban and rural sites in North China Plain in winter 2019 to
265 characterize the chemical composition and mixing state of BC-containing particles and their impacts on light absorption enhancement. Our results showed that BC-containing particles were primarily mixed with OC, NO_3 and SO_4 at both sites while the rural site showed much higher fraction of OC and nitrate coated BC (36% vs. 15 – 20%). The increased BC particles internally mixed with large amount of NO_3 was mainly due to the effect of clean air action that reduced much more sulfate than nitrate in $PM_{2.5}$. The average contribution of SOA to the OC coated on BC was about twice than that of POA in BJ, while
270 both of them contributed similarly to the OC coating in GC. In addition, OC and metals were likely as filler materials internally mixed with fresh BC and did not induce much light absorption enhancement at the urban site, while they were coated on fresh BC and induced light absorption enhancement (~ 1.2) at the rural site.

By analyzing the variations of BC mixing state in different environments, we found that BC particles were primarily mixed with NO_3 as the increase of RH at both urban and rural sites. In particular, the BC emitted from biomass burning was first
275 mixed with NO_3 at relatively high RH level and then mixed with both nitrate and sulfate after further aging. Comparatively, the BC emitted from coal combustion was more internally mixed with OC and NO_3 , and then mixed with sulfate ($BCOC_{NS}$) with similar processes. Thus, higher coal combustion emissions can result in the increase in the fraction of $BCOC_N$ as the



increase of RH at the rural site, while BC_N was generally the dominant BC-containing particles in Beijing. Although BC particles presented different mixing state in different environments, E_{abs} showed a similar evolutionary dependence on the changes in mixing state, i.e., from the small E_{abs} (1.06~1.11) with fresh BC emissions to above 1.30 after aged and internally mixed with nitrate and OC-nitrate (BC_N and $BCOC_N$), and to above 1.40 after further aging with the sulfate involved.

Data availability. The data in this study are available from the authors upon request (sunyele@mail.iap.ac.cn).

Author contributions. YS and JS designed the research. JS, CX, WX, CC and ZL conducted the measurements. JS, WX, CC, ZW and YL analyzed the data. CX, LL, XD, FH, XP, NM, WX, PF and ZiW reviewed and commented on the paper. JS and YS wrote the paper.

Competing interests. The authors declare that they have no conflict of interest.

Acknowledgements. This work was supported by the National Natural Science Foundation of China (9204430003, 42061134008).

References

- Bond, T. C. and Bergstrom, R. W.: Light absorption by carbonaceous particles: an investigative review, *Aerosol Sci. Technol.*, 40, 27-67, 10.1080/02786820500421521, 2006.
- Bond, T. C., Doherty, S. J., Fahey, D. W., Forster, P. M., Berntsen, T., DeAngelo, B. J., Flanner, M. G., Ghan, S., Kärcher, B., Koch, D., Kinne, S., Kondo, Y., Quinn, P. K., Sarofim, M. C., Schultz, M. G., Schulz, M., Venkataraman, C., Zhang, H., Zhang, S., Bellouin, N., Guttikunda, S. K., Hopke, P. K., Jacobson, M. Z., Kaiser, J. W., Klimont, Z., Lohmann, U., P. S. J., Shindell, D., Storelvmo, T., Warren, S. G., and Zender, C. S.: Bounding the role of black carbon in the climate system: a scientific assessment, *J. Geophys. Res.-Atmos.*, 118, 5380-5552, 10.1002/jgrd.50171, 2013.
- Buseck, P. R., Adachi, K., Andras, G., Tompa, E., and Mihaly, P.: Ns-Soot: a material-based term for strongly light-absorbing carbonaceous particles, *Aerosol Sci. Technol.*, 48, 777-788, 10.1080/02786826.2014.919374, 2014.
- Cappa, C. D., Onasch, T. B., Massoli, P., Worsnop, D. R., Bates, T. S., Cross, E. S., Davidovits, P., Hakala, J., Hayden, K. L., and Jobson, B. T.: Radiative absorption enhancements due to the mixing state of atmospheric black carbon, *Science*, 337, 6098, 10.1126/science.1223447, 2012.
- Cappa, C. D., Zhang, X., Russell, L. M., Collier, S., Lee, A. K. Y., Chen, C.-L., Betha, R., Chen, S., Liu, J., Price, D. J., Sanchez, K. J., McMeeking, G. R., Williams, L. R., Onasch, T. B., Worsnop, D. R., Abbatt, J., and Zhang, Q.: Light



- absorption by ambient black and brown carbon and its dependence on black carbon coating state for two California, USA,
305 cities in winter and summer, *J. Geophys. Res.-Atmos.*, 124, 1550-1577, 10.1029/2018jd029501, 2019.
- Chen, C., Qiu, Y., Weiqi, X., He, Y., Li, Z., Sun, J., Ma, N., Xu, W., Pan, X., Fu, P., Wang, Z., and Sun, Y.: Primary emissions
and secondary aerosol processing during wintertime in rural area of North China Plain, *J. Geophys. Res.-Atmos.*, <under
review>, 2021.
- Chen, L., Zhang, F., Yan, P., Wang, X., Sun, L., Li, Y., Zhang, X., Sun, Y., and Li, Z.: The large proportion of black carbon
310 (BC)-containing aerosols in the urban atmosphere, *Environ. Pollut.*, 263, 114507, 10.1016/j.envpol.2020.114507, 2020a.
- Chen, Y. and Bond, T. C.: Light absorption by organic carbon from wood combustion, *Atmos. Chem. Phys.*, 10, 1773-1787,
2010.
- Chen, Y., Tian, M., Huang, R.-J., Shi, G., Wang, H., Peng, C., Cao, J., Wang, Q., Zhang, S., Guo, D., Zhang, L., and Yang,
F.: Characterization of urban amine-containing particles in southwestern China: seasonal variation, source, and processing,
315 *Atmos. Chem. Phys.*, 19, 3245-3255, 10.5194/acp-19-3245-2019, 2019.
- Chen, Y., Cai, J., Wang, Z., Peng, C., Yao, X., Tian, M., Han, Y., Shi, G., Shi, Z., Liu, Y., Yang, X., Zheng, M., Zhu, T., He,
K., Zhang, Q., and Yang, F.: Simultaneous measurements of urban and rural particles in Beijing – Part 1: chemical
composition and mixing state, *Atmos. Chem. Phys.*, 20, 9231-9247, 10.5194/acp-20-9231-2020, 2020b.
- Chen, Y., Kozlovskiy, V., Du, X., Lv, J., Nikiforov, S., Yu, J., Kolosov, A., Gao, W., Zhou, Z., Huang, Z., and Li, L.: Increase
320 of the particle hit rate in a laser single-particle mass spectrometer by pulse delayed extraction technology, *Atmos. Meas.
Tech.*, 13, 941-949, 10.5194/amt-13-941-2020, 2020c.
- Chylek, P. and Wong, J.: Effect of aerosols on global budget, *Geophys. Res. Lett.*, 22, 929-931, 1995.
- Ding, A. J., Huang, X., Nie, W., Sun, J. N., Kerminen, V. M., Petäjä, T., Su, H., Cheng, Y. F., Yang, X. Q., Wang, M. H., Chi,
X. G., Wang, J. P., Virkkula, A., Guo, W. D., Yuan, J., Wang, S. Y., Zhang, R. J., Wu, Y. F., Song, Y., Zhu, T.,
325 Zilitinkevich, S., Kulmala, M., and Fu, C. B.: Enhanced haze pollution by black carbon in megacities in China, *Geophys.
Res. Lett.*, 43, 2873-2879, 10.1002/2016gl067745, 2016.
- Fuller, K. A., Malm, W. C., and Kreidenweis, S. M.: Effects of mixing on extinction by carbonaceous particles, *J. Geophys.
Res.*, 104, 15941-15954, 10.1029/1998jd100069, 1999.
- Healy, R. M., Hellebust, S., Kourtev, I., Allanic, A., O'Connor, I. P., Bell, J. M., Healy, D. A., Sodeau, J. R., and Wenger,
330 J. C.: Source apportionment of PM_{2.5} in Cork Harbour, Ireland using a combination of single particle mass spectrometry
and quantitative semi-continuous measurements, *Atmos. Chem. Phys.*, 10, 9593-9613, 10.5194/acp-10-9593-2010, 2010.
- Healy, R. M., Sciare, J., Poulain, L., Kamili, K., Merkel, M., Müller, T., Wiedensohler, A., Eckhardt, S., Stohl, A., Sarda-
Estève, R., McGillicuddy, E., and Connor, I. P., Sodeau, J. R., and Wenger, J. C.: Sources and mixing state of size-
resolved elemental carbon particles in a European megacity: Paris, *Atmos. Chem. Phys.*, 12, 1681-1700, 10.5194/acp-12-
335 1681-2012, 2012.
- IPCC: Climate Change 2013: The Physical Science Basis. Contribution of Working Group I to the Fifth Assessment Report
of the Intergovernmental Panel on Climate Change [Stocker, T.F., D. Qin, G.-K. Plattner, M. Tignor, S.K. Allen, J.
Boschung, A. Nauels, Y. Xia, V. Bex and P.M. Midgley (eds.)]. Cambridge University Press, Cambridge, United Kingdom
and New York, NY, USA, 1535 pp, doi:10.1017/CBO9781107415324, 2013.



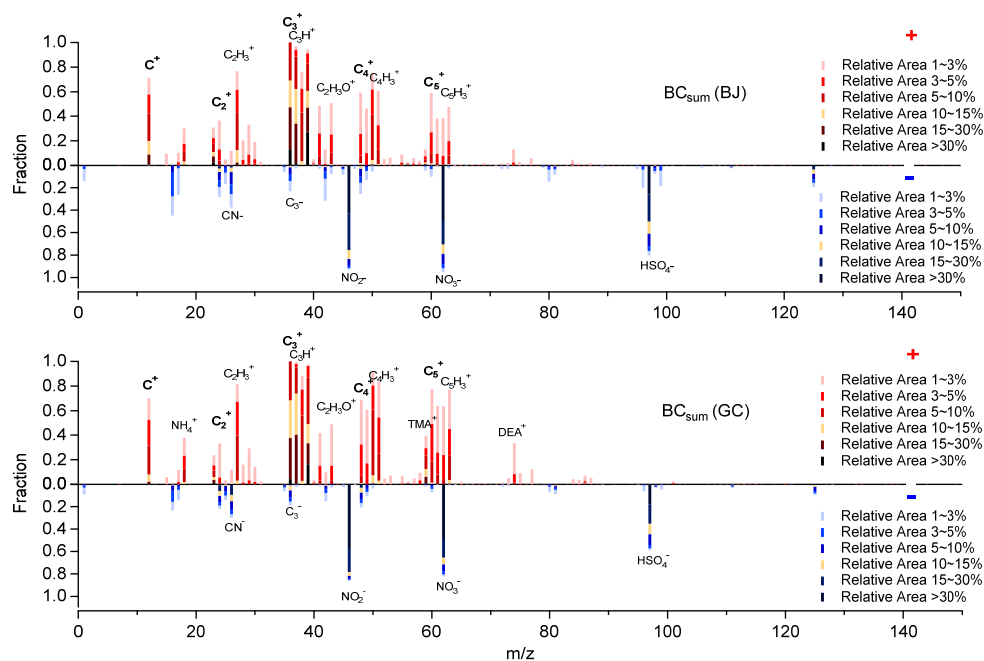
- 340 Kahnert, M.: On the discrepancy between modeled and measured mass absorption cross sections of light absorbing carbon aerosols, *Aerosol Sci. Technol.*, 44, 453-460, 10.1080/02786821003733834, 2010.
- Lack, D. A. and Cappa, C. D.: Impact of brown and clear carbon on light absorption enhancement, single scatter albedo and absorption wavelength dependence of black carbon, *Atmos. Chem. Phys.*, 10, 4207-4220, 10.5194/acp-10-4207-2010, 2010.
- 345 Lee, A. K. Y., Willis, M. D., Healy, R. M., Onasch, T. B., and Abbatt, J. P. D.: Mixing state of carbonaceous aerosol in an urban environment: single particle characterization using the soot particle aerosol mass spectrometer (SP-AMS), *Atmos. Chem. Phys.*, 15, 1823-1841, 10.5194/acp-15-1823-2015, 2015.
- Lei, L., Zhou, W., Chen, C., He, Y., Li, Z., Sun, J., Tang, X., Fu, P., Wang, Z., and Sun, Y.: Long-term characterization of aerosol chemistry in cold season from 2013 to 2020 in Beijing, China, *Environ. Pollut.*, 268, 115952, 10.1016/j.envpol.2020.115952, 2020.
- 350 Li, L., Huang, Z., Dong, J., Li, M., Gao, W., Nian, H., Fu, Z., Zhang, G., Bi, X., Cheng, P., and Zhou, Z.: Real time bipolar time-of-flight mass spectrometer for analyzing single aerosol particles, *Int. J. Mass Spectrom.*, 303, 118-124, 10.1016/j.ijms.2011.01.017, 2011.
- Li, W., Sun, J., Xu, L., Shi, Z., Riemer, N., Sun, Y., Fu, P., Zhang, J., Lin, Y., Wang, X., Shao, L., Chen, J., Zhang, X., Wang, Z., and Wang, W.: A conceptual framework for mixing structures in individual aerosol particles, *J. Geophys. Res.-Atmos.*, 121, 13,784-713,798, 10.1002/2016jd025252, 2016a.
- 355 Li, W. J., Shao, L. Y., Zhang, D. Z., Ro, C. U., Hu, M., Bi, X. H., Geng, H., Matsuki, A., Niu, H. Y., and Chen, J. M.: A review of single aerosol particle studies in the atmosphere of East Asia: morphology, mixing state, source, and heterogeneous reactions, *J. Clean Prod.*, 112, 1330-1349, 10.1016/j.jclepro.2015.04.050, 2016b.
- 360 Liu, D., Whitehead, J., Alfara, M. R., Reyes-Villegas, E., Spracklen, Dominick V., Reddington, Carly L., Kong, S., Williams, Paul I., Ting, Y.-C., Haslett, S., Taylor, Jonathan W., Flynn, Michael J., Morgan, William T., McFiggans, G., Coe, H., and Allan, James D.: Black-carbon absorption enhancement in the atmosphere determined by particle mixing state, *Nat. Geosci.*, 10, 184-188, 10.1038/ngeo2901, 2017.
- 365 Liu, D., Joshi, R., Wang, J., Yu, C., Allan, J. D., Coe, H., Flynn, M. J., Xie, C., Lee, J., Squires, F., Kotthaus, S., Grimmond, S., Ge, X., Sun, Y., and Fu, P.: Contrasting physical properties of black carbon in urban Beijing between winter and summer, *Atmos. Chem. Phys.*, 19, 6749-6769, 10.5194/acp-19-6749-2019, 2019.
- Liu, S., Aiken, A. C., Gorkowski, K., Dubey, M. K., Cappa, C. D., Williams, L. R., Herndon, S. C., Massoli, P., Fortner, E., and Chhabra, P. S.: Enhanced light absorption by mixed source black and brown carbon particles in UK winter, *Nat. Commun.*, 6, 8435-8435, 10.1080/02786820500421521, 2015.
- 370 Petit, J. E., Favez, O., Sciare, J., Canonaco, F., Croteau, P., Močnik, G., Jayne, J., Worsnop, D., and Leoz-Garziandia, E.: Submicron aerosol source apportionment of wintertime pollution in Paris, France by double positive matrix factorization (PMF2) using an aerosol chemical speciation monitor (ACSM) and a multi-wavelength Aethalometer, *Atmos. Chem. Phys.*, 14, 13773-13787, 10.5194/acp-14-13773-2014, 2014.
- 375 Pratt, K. A. and Prather, K. A.: Mass spectrometry of atmospheric aerosols-recent developments and applications. Part II: on-line mass spectrometry techniques, *Mass Spectrom. Rev.*, 31, 17-48, 10.1002/mas.20330, 2012.



- Shen, W., Dai, X., Huang, Z., Hou, Z., Cai, W., Du, X., Zhou, Z., Li, M., and Li, L.: Improvement of the dynamic range of data acquisition system in single particle mass spectrometry, *J. Chinese Cinemas.*, 039, 331-336, 2018.
- Silva, P. J., Liu, D. Y., Noble, C. A., and Prather, K. A.: Size and chemical characterization of individual particles resulting from biomass burning of local Southern California species, *Environ. Sci. Technol.*, 33, 3068-3076, 10.1021/es980544p, 1999.
- 380 Song, X. H., Hopke, P. K., Fergenson, D. P., and Prather, K. A.: Classification of single particles analyzed by ATOFMS using an artificial neural network, *ART-2A, Anal. Chem.*, 71, 860-865, 10.1021/ac9809682, 1999.
- Sun, J., Xie, C., Xu, W., Chen, C., Ma, N., Xu, W., Lei, L., Li, Z., He, Y., Qiu, Y., Wang, Q., Pan, X., Su, H., Cheng, Y., Wu, C., Fu, P., Wang, Z., and Sun, Y.: Light absorption of black carbon and brown carbon in winter in North China Plain: comparisons between urban and rural sites, *Sci. Total Environ.*, 770, 10.1016/j.scitotenv.2020.144821, 2021.
- 385 Thamban, N. M., Tripathi, S. N., Moosakutty, S. P., Kuntamukkala, P., and Kanawade, V. P.: Internally mixed black carbon in the Indo-Gangetic Plain and its effect on absorption enhancement, *Atmos. Res.*, 197, 211-223, 10.1016/j.atmosres.2017.07.007, 2017.
- Vignati, E., Karl, M., Krol, M., Wilson, J., Stier, P., and Cavalli, F.: Sources of uncertainties in modelling black carbon at the global scale, *Atmos. Chem. Phys.*, 10, 2595-2611, 10.5194/acp-10-2595-2010, 2010.
- 390 Wang, Q., Cao, J., Han, Y., Wang, G., Li, G., Wang, Y., Dai, W., Zhang, R., Zhou, Y., and Psi, V.: Mixing state of black carbon aerosol in a heavily polluted urban area of China: implications for light absorption enhancement, *Aerosol Sci. Technol.*, 48, 689-697, 2014.
- Wang, Q., Li, L., Zhou, J., Ye, J., Dai, W., Liu, H., Zhang, Y., Zhang, R., Tian, J., Chen, Y., Wu, Y., Ran, W., and Cao, J.: Measurement report: source and mixing state of black carbon aerosol in the North China Plain: implications for radiative effect, *Atmos. Chem. Phys.*, 20, 15427-15442, 10.5194/acp-20-15427-2020, 2020.
- 395 Xie, C., Xu, W., Wang, J., Liu, D., Ge, X., Zhang, Q., Wang, Q., Du, W., Zhao, J., and Zhou, W.: Light absorption enhancement of black carbon in urban Beijing in summer, *Atmos. Environ.*, 213, 499-504, 2019a.
- Xie, C., Xu, W., Wang, J., Wang, Q., Liu, D., Tang, G., Chen, P., Du, W., Zhao, J., Zhang, Y., Zhou, W., Han, T., Bian, Q., 400 Li, J., Fu, P., Wang, Z., Ge, X., Allan, J., Coe, H., and Sun, Y.: Vertical characterization of aerosol optical properties and brown carbon in winter in urban Beijing, China, *Atmos. Chem. Phys.*, 19, 165-179, 10.5194/acp-19-165-2019, 2019b.
- Xie, C., He, Y., Lei, L., Zhou, W., Liu, J., Wang, Q., Xu, W., Qiu, Y., Zhao, J., Sun, J., Li, L., Li, M., Zhou, Z., Fu, P., Wang, Z., and Sun, Y.: Contrasting mixing state of black carbon-containing particles in summer and winter in Beijing, *Environ. Pollut.*, 263, 10, 10.1016/j.envpol.2020.114455, 2020.
- 405 Xu, W., Chen, C., Qiu, Y., Xie, C., Chen, Y., Ma, N., Xu, W., Fu, P., Wang, Z., Pan, X., Zhu, J., Ng, N. L., and Sun, Y.: Size-resolved characterization of organic aerosol in the North China Plain: new insights from high resolution spectral analysis, *Environ. Sci.: Atmos.*, 1, 346-358, 10.1039/d1ea00025j, 2021.
- Yang, J., Ma, S., Gao, B., Li, X., Zhang, Y., Cai, J., Li, M., Yao, L., Huang, B., and Zheng, M.: Single particle mass spectral signatures from vehicle exhaust particles and the source apportionment of on-line PM_{2.5} by single particle aerosol mass spectrometry, *Sci. Total Environ.*, 593-594, 310-318, 10.1016/j.scitotenv.2017.03.099, 2017.
- 410



- Zhang, G., Bi, X., Chan, L. Y., Li, L., Wang, X., Feng, J., Sheng, G., Fu, J., Li, M., and Zhou, Z.: Enhanced trimethylamine-containing particles during fog events detected by single particle aerosol mass spectrometry in urban Guangzhou, China, *Atmos. Environ.*, 55, 121-126, 10.1016/j.atmosenv.2012.03.038, 2012.
- 415 Zhang, Q., Zheng, Y., Tong, D., Shao, M., Wang, S., Zhang, Y., Xu, X., Wang, J., He, H., Liu, W., Ding, Y., Lei, Y., Li, J., Wang, Z., Zhang, X., Wang, Y., Cheng, J., Liu, Y., Shi, Q., Yan, L., Geng, G., Hong, C., Li, M., Liu, F., Zheng, B., Cao, J., Ding, A., Gao, J., Fu, Q., Huo, J., Liu, B., Liu, Z., Yang, F., He, K., and Hao, J.: Drivers of improved PM_{2.5} air quality in China from 2013 to 2017, *Proc. Natl. Acad. Sci. U. S. A.*, 116, 24463-24469, 10.1073/pnas.1907956116, 2019.
- 420 Zhang, X., Kim, H., Parworth, C. L., Young, D. E., Zhang, Q., Metcalf, A. R., and Cappa, C. D.: Optical properties of wintertime aerosols from residential wood burning in Fresno, CA: results from DISCOVER-AQ 2013, *Environ. Sci. Technol.*, 50, 1681-1690, 10.1021/acs.est.5b04134, 2016.
- Zhang, Y., Wang, X., Chen, H., Yang, X., Chen, J., and Allen, J. O.: Source apportionment of lead-containing aerosol particles in Shanghai using single particle mass spectrometry, *Chemosphere*, 74, 501-507, 10.1016/j.chemosphere.2008.10.004, 2009.
- 425 Zhang, Y., Favez, O., Canonaco, F., Liu, D., Močnik, G., Amodeo, T., Sciare, J., Prévôt, A. S. H., Gros, V., and Albinet, A.: Evidence of major secondary organic aerosol contribution to lensing effect black carbon absorption enhancement, *npj Clim. Atmos. Sci.*, 1, 1-8, 10.1038/s41612-018-0056-2, 2018.
- Zhang, Y., Liu, H., Lei, S., Xu, W., Tian, Y., Yao, W., Liu, X., Liao, Q., Li, J., Chen, C., Sun, Y., Fu, P., Xin, J., Cao, J., Pan, X., and Wang, Z.: Mixing state of refractory black carbon in fog and haze at rural sites in winter on the North China Plain, *Atmos. Chem. Phys. Discuss.* [preprint], in review, 2021.
- 430 Zhong, Q. E., Cheng, C., Wang, Z., Li, L., Li, M., Ge, D., Wang, L., Li, Y., Nie, W., Chi, X., Ding, A., Yang, S., Chen, D., and Zhou, Z.: Diverse mixing states of amine-containing single particles in Nanjing, China, *Atmos. Chem. Phys. Discuss.* [preprint], in review, 10.5194/acp-2021-593, 2021.
- Zhou, W., Gao, M., He, Y., Wang, Q., Xie, C., Xu, W., Zhao, J., Du, W., Qiu, Y., Lei, L., Fu, P., Wang, Z., Worsnop, D. R., Zhang, Q., and Sun, Y.: Response of aerosol chemistry to clean air action in Beijing, China: insights from two-year ACSM measurements and model simulations, *Environ. Pollut.*, 255, 113345, 2019.
- 435 Zhu, S., Li, L., Wang, S., Li, M., Liu, Y., Lu, X., Chen, H., Wang, L., Chen, J., Zhou, Z., Yang, X., and Wang, X.: Development of an automatic linear calibration method for high-resolution single-particle mass spectrometry: improved chemical species identification for atmospheric aerosols, *Atmos. Meas. Tech.*, 13, 4111-4121, 10.5194/amt-13-4111-2020, 2020.



445 **Figure 1.** The digital positive and negative mass spectra of BC-containing particles in Beijing and Gucheng. The ion height indicates its number fraction in the BC-containing dataset (i.e., the number ratio of BC-containing particles with the corresponding ion detected in mass spectra to the total BC-containing particles). The color bars represent each relative peak area corresponding to a specific fraction in individual particles.

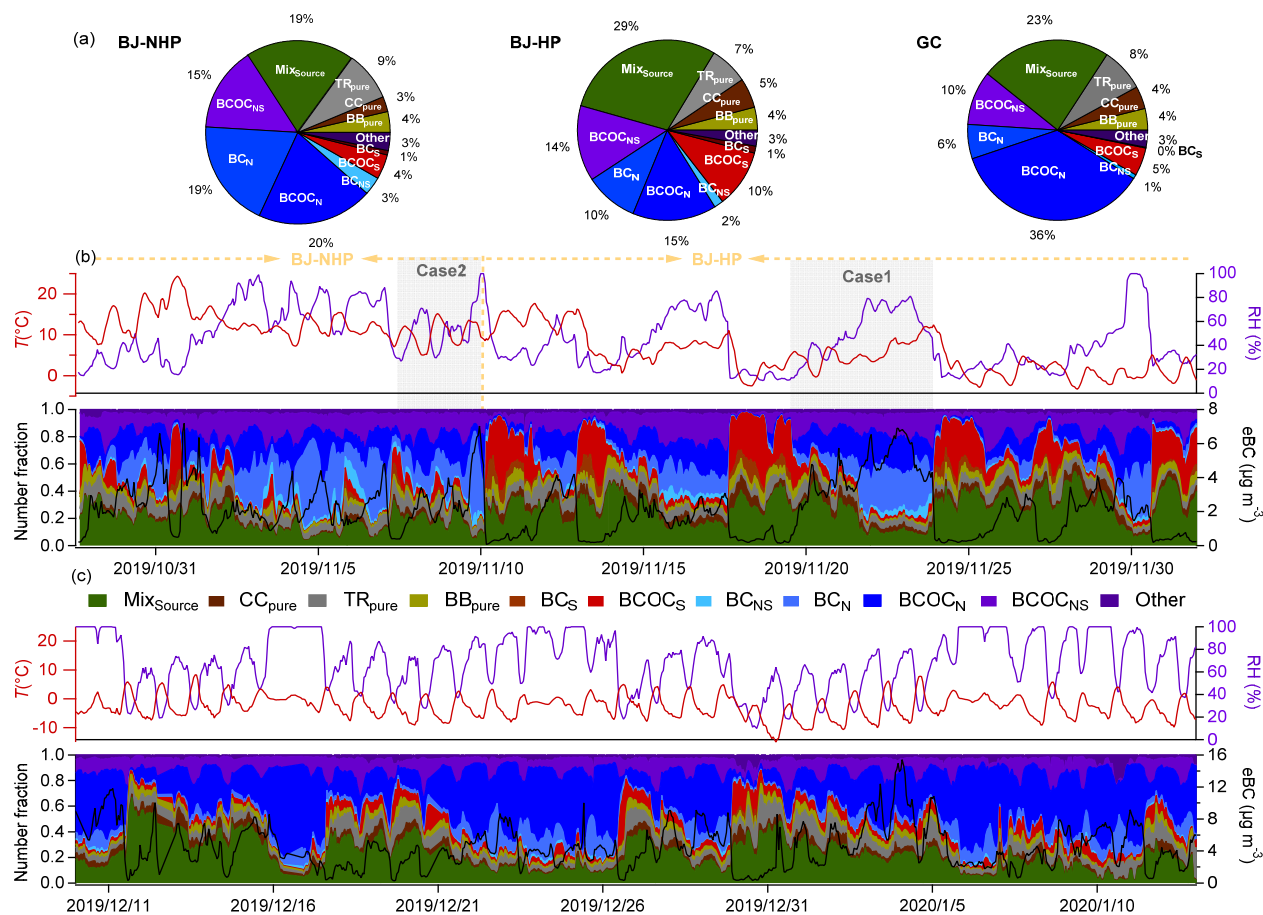


Figure 2. (a) Relative number abundance distribution of major BC-containing particle types during different periods. Temporal variation of ambient temperature (T), relative humidity (RH) and number fractions of BC-containing particle types in (b) Beijing and (c) Gucheng.

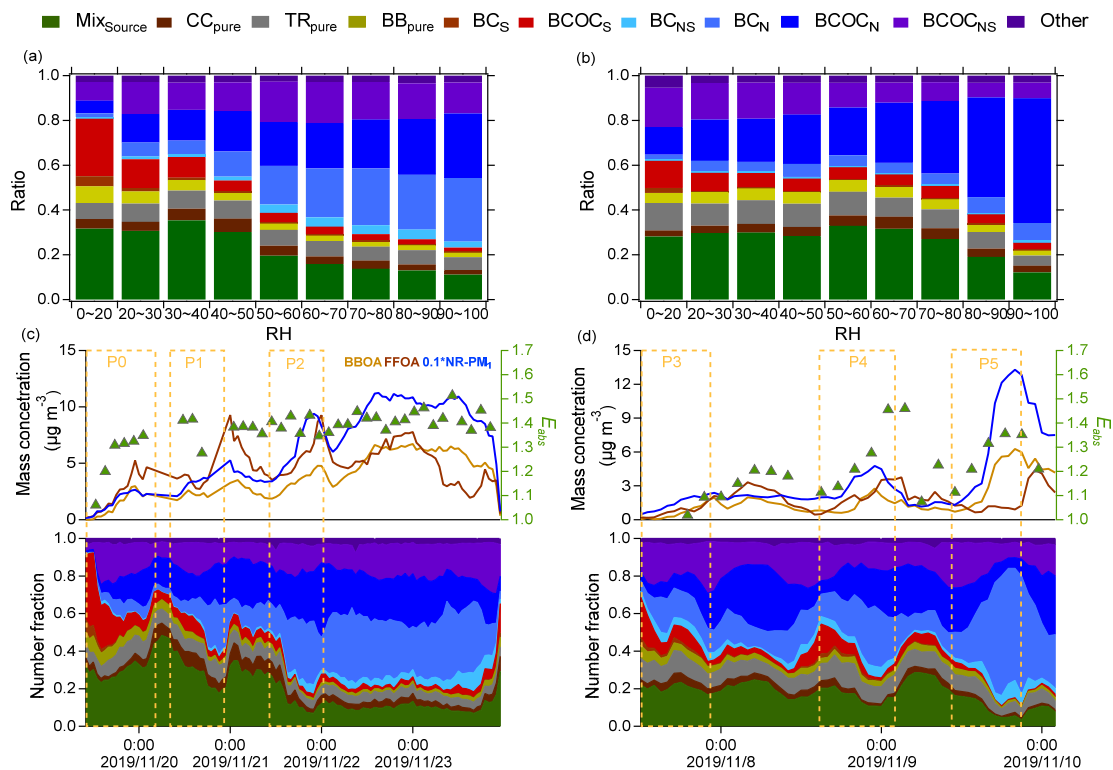
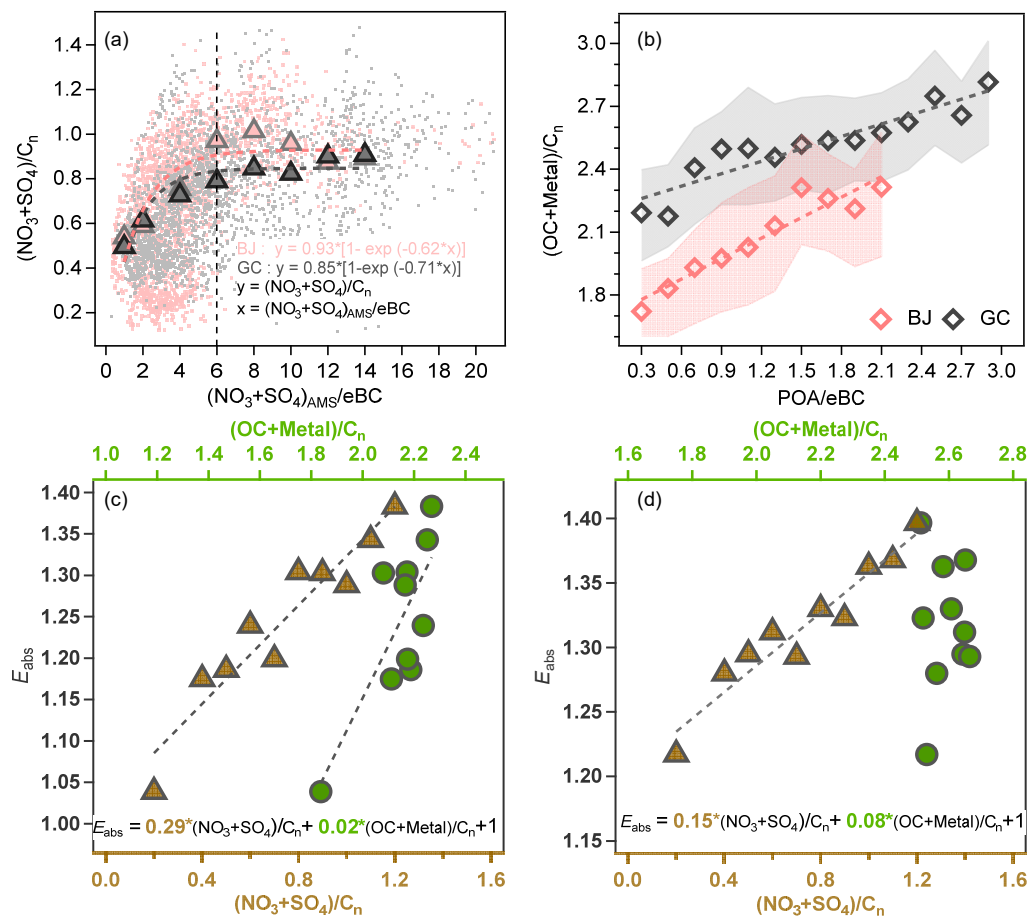
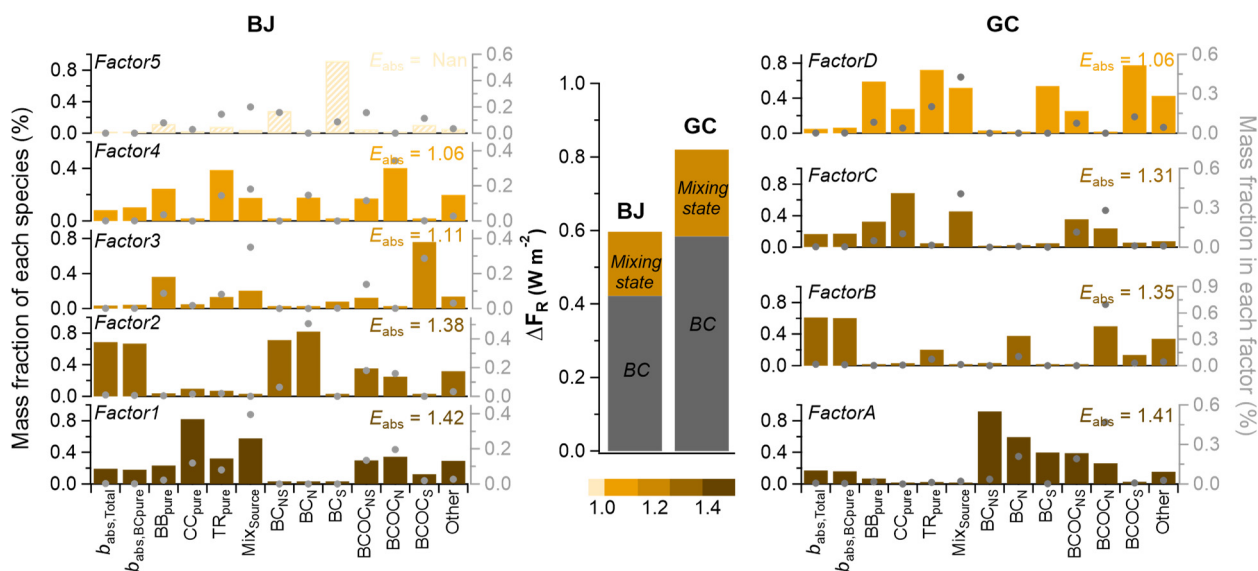


Figure 3. Variations of number fractions of BC-containing particle types with RH in (a) Beijing and (b) Gucheng. Temporal variations of E_{abs} , number fractions of BC-containing particle types and mass concentration of species during polluted (c) Case1 and (d) Case2.



455

Figure 4. Relationships between peak area ratios and mass concentration ratios: (a) $(\text{NO}_3 + \text{SO}_4)/C_n$ vs. $(\text{NO}_3 + \text{SO}_4)_{\text{AMS}}/e\text{BC}$ and (b) $(\text{OC} + \text{Metal})/C_n$ vs. $\text{POA}/e\text{BC}$. Relationships between E_{abs} and peak area ratios of coating materials ($(\text{NO}_3 + \text{SO}_4)/C_n$ and $(\text{OC} + \text{Metal})/C_n$) in (c) Beijing and (d) Gucheng.



460 **Figure 5.** Factor profiles and their contributions to each factor identified by the positive matrix factorization model in BJ and GC.

$b_{\text{abs, total}}$ and $b_{\text{abs, BCpure}}$ represent light absorption (Mm^{-1}) of coated BC particles and pure BC, respectively. BC types e.g., BB_{pure} in units of count.